Organic & Biomolecular Chemistry

Accepted Manuscript

This article can be cited before page numbers have been issued, to do this please use: Y. Kishimoto, A. Fujii, O. Nakagawa, T. Nagata, T. Yokota, Y. Hari and S. Obika, *Org. Biomol. Chem.*, 2017, DOI: 10.1039/C7OB01874F.

ROYAL SOCIETY OF CHEMISTRY

rsc.li/obc

View Article Online
DOI: 10.1039/C7OB01874F

PAPER

Synthesis and thermal stabilities of oligonucleotides containing 2′-*O*,4′-*C*-methylene bridged nucleic acid with a phenoxazine base

Received 00th January 20xx,
Accepted 00th January 20xx

DOI: 10.1039/x0xx00000x

www.rsc.org/

Yuki Kishimoto,[a,b] Akane Fujii,[a,b] Osamu Nakagawa,*[a,b] Tetsuya Nagata,[b,c] Takanori Yokota,[b,c] Yoshiyuki Hari,[d] and Satoshi Obika*[a,b]

We designed and synthesized a novel artificial 2′-*O*,4′-*C*-methylene bridged nucleic acid (2′,4′-BNA/LNA) with a phenoxazine nucleobase and named this compound BNAP. Oligodeoxynucleotide (ODN) containing BNAP showed higher binding affinities toward complementary DNA and RNA as compared to ODNs bearing 2′,4′-BNA/LNA with 5-methylcytosine or 2′-deoxyribonucleoside with phenoxazine. Thermodynamic analysis revealed that BNAP exhibits properties associated with the phenoxazine moiety in DNA/DNA duplexes and characteristics associated with the 2′,4′-BNA/LNA moiety in DNA/RNA duplexes.

Introduction

Various artificial nucleic acids have been developed for application in oligonucleotide technologies such as antisense/antigene, small interfering RNA, aptamers, and single nucleotide polymorphism (SNP) analysis.[1)] These modified nucleic acids exhibit useful properties, including improved duplex-forming ability, stability against enzymatic degradation, and accurate base discrimination. One of the most promising modified nucleic acids is 2′-*O*,4′-*C*-methylene bridged nucleic acid (abbreviated as either 2′,4′-BNA or LNA) independently developed by our laboratory[2)] and Wengel's group[3)]. 2′,4′-BNA/LNA is strictly locked into the N-type sugar conformation (C3′-*endo*) and shows high duplex-forming ability and gene knockdown efficiency *in vivo* (Figure 1, a). The design concept behind 2′,4′-BNA/LNA is to prevent entropy loss by pre-organizing the structure into the N-type sugar conformation preferred in A-form duplexes. Based on this concept, we have developed a series of 2′,4′-bridged nucleic acids such as AmNA[4)], GuNA[5)], scpBNA[6)], and SeLNA[7)]. In addition, various artificial nucleobases can be introduced into the original 2′,4′-BNA/LNA in place of the four natural bases (A, G, C and T) and these analogues exhibit novel functionalities and work effectively in oligonucleotide technology applications.[8)] For example, we have developed 2′,4′-BNA/LNAs with several artificial nucleobases for application in antigene strategies using triplex-forming oligonucleotides (TFOs).[9)] TFOs containing 2′,4′-BNA/LNA analogues exhibited improved recognition ability toward CG or TA base pairs that could not be recognized by natural nucleobases.

Here, we focused on the nucleobase modification of 2′,4′-BNA/LNA. The artificial phenoxazine base is a tricyclic cytosine analogue that shows high binding affinity towards complementary guanine (ΔT_m: approximately +6°C compared with cytosine) (Figure 1, b)[10)] due to effective π-π stacking interaction of the tricyclic aromatic ring with the flanking nucleobase in an oligonucleotide.[10a,b)] Pyrimidine bases in the 5′-flanking site interact effectively with phenoxazine. The phenoxazine base and its 5-sulfur analogue (phenothiazine base) have promising properties such as fluorescence[11)], enzymatic stability[12)] and polymerase recognition[13)]. Moreover, a phenoxazine derivative bearing an aminoethoxy unit at 9-position (named G-clamp) is well-studied.[14)]

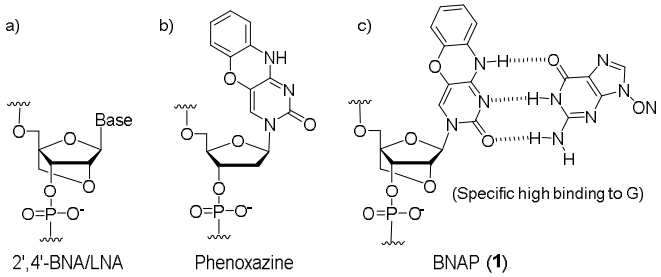

Figure 1. Design of 2′,4′-bridged nucleic acid with a phenoxazine base (BNAP).

[a] Graduate School of Pharmaceutical Sciences, Osaka University, 1-6 Yamadaoka, Suita, Osaka 565-0871, Japan.
[b] Core Research for Evolutional Science and Technology (CREST), Japan Sciences and Technology Agency (JST), 7 Gobancho, Chiyoda-ku, Tokyo 102-0076, Japan.
[c] Department of Neurology and Neurological Science, Graduate School of Medical and Dental Sciences, Tokyo Medical and Dental University, 1-5-45 Yushima, Bunkyo-ku, Tokyo 113-8519, Japan.
[d] Faculty of Pharmaceutical Sciences, Tokushima Bunri University, Nishihama, Yamashiro-cho, Tokushima 770-8514, Japan
E-mail: obika@phs.osaka-u.ac.jp (S.Obika), osamu_nakagawa@phs.osaka-u.ac.jp (O. Nakagawa)

† Footnotes relating to the title and/or authors should appear here.
Electronic Supplementary Information (ESI) available: [details of any supplementary information available should be included here]. See DOI: 10.1039/x0xx00000x

Both 2′,4′-BNA/LNA and the phenoxazine base improve the duplex-forming ability of oligonucleotides but through different molecular mechanisms. Therefore, combining these two moieties could be a good strategy for the design of new oligonucleotides with high binding affinity. We designed 2′,4′-Bridged Nucleic Acid with Phenoxazine base (abbreviated BNAP) and here describe its synthesis and properties (Figure 1, c).

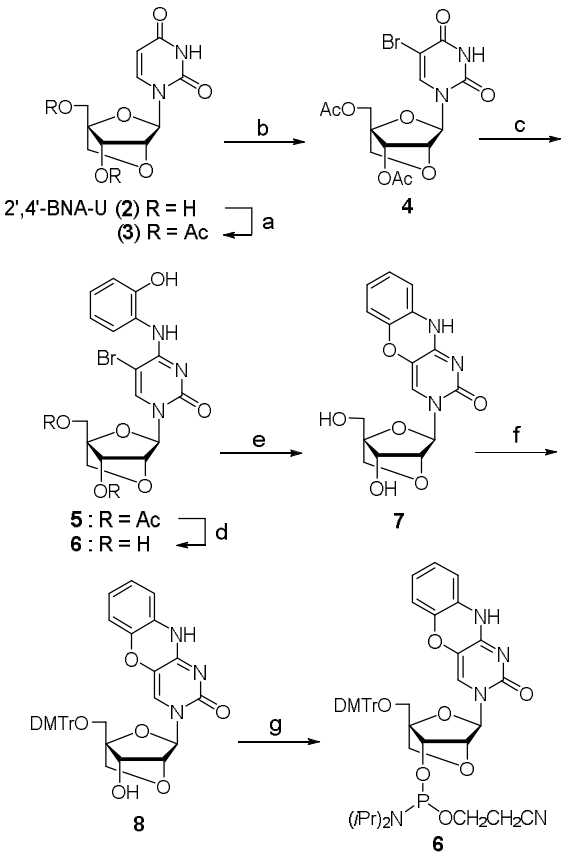

Scheme 1. Synthesis of BNAP phosphoramidite.
Reagents and conditions: (a) Ac_2O, pyridine, rt, 7 h (99%); (b) NBS, DMF, 0°C→rt, 2.5 h (81%); (c) PPh_3, CCl_4, CH_2Cl_2, reflux, 2 h, then 2-aminophenol, DBU, rt, 12 h; (d) 7 M NH_3 in MeOH, rt, 2 h (81% in 2 steps); (e) DBU, EtOH, reflux, 30 h (59%); (f) DMTrCl, AgOTf, 2,6-lutidine, CH_2Cl_2, 0°C, 3 h (58%); (g) *i*-$Pr_2NP(Cl)OCH_2CH_2CN$, DIPEA, CH_2Cl_2, rt, 3 h, (74%).

Results

Synthesis of BNAP nucleoside and incorporation into oligodeoxynucleotides

As shown in Scheme 1, the synthesis of BNAP nucleoside started with known 2′,4′-BNA/LNA-uridine (**2**).[15] After protection of the 3′,5′-hydroxy groups of **2** with acetyl groups, **3** was brominated at C-5 with *N*-bromosuccinimide (NBS) to give **4**. The 4-carbonyl group of **4** was chlorinated using the Appel reaction,[14a] then reacted with 2-aminophenol and 1,8-diazabicyclo[5.4.0]undec-7-ene (DBU) to afford **5**. After deprotection of the 3′,5′-acetyl groups, formation of the phenoxazine skeleton with **6** was achieved in 59% yield using basic conditions with DBU in ethanol at reflux. Next, the 5′-hydroxy group of **7** was protected with a 4,4′-dimethoxytrityl (DMTr) group to give **8**. The reaction under typical conditions (DMTrCl in pyridine) did not proceed effectively whereas DMTrOTf successfully gave the desired product. Finally, the 3′-hydroxy group of **8** was phosphitylated to afford phosphoramidite **9**.

Subsequently, the phosphoramidite **9** was satisfactorily incorporated into oligodeoxynucleotides (ODNs) using an automated DNA synthesizer by following the standard phosphoramidite protocol with a prolonged coupling time, using 5-[3,5-bis(trifluoromethyl)phenyl]-1*H*-tetrazole (Activator 42®) as the activator. The synthesized ODNs were cleaved from the controlled pore glass (CPG)-supported columns using a solution of aqueous methylamine and aqueous ammonia (v/v, 1/1) at 65°C for 10 min, purified by reverse-phase HPLC, and their composition was confirmed by MALDI-TOF-MS spectrometry (Table 1).

The chemical stabilities of ODNs containing BNAP (**B**) (termed **B**-ODNs) were similar to that of the corresponding ODNs containing 2′-deoxyribonucleotide with phenoxazine (**P**) (**P**-ODNs). The **B**-ODNs were unstable in the aqueous ammonia solution conditions (10 h at 55°C) used in typical deprotection/cleavage steps, and therefore deprotection was conducted with the above aqueous ammonia/methylamine (v/v, 1/1) solution at 65°C for 10 min. It is known that phenoxazine base exhibits fluorescence (Em: approximately 450 nm, Ex: 365 nm).[11f,h] The **B**-ODNs showed fluorescence similar to **P**-ODNs (see Supporting Information, Figure S3).

Table 1. MALDI-TOF mass data of ODNs containing BNAP.

Sequences (**B**: BNAP)	MALDI-TOF Mass	
	Calcd. $(M-H)^-$	Found
5′-d(GCGTT**B**TTTGCT)-3′	3735.5	3735.2
5′-d(GCGTC**B**ATTGCT)-3′	3729.5	3728.2
5′-d(GCGTC**B**CTTGCT)-3′	3705.4	3705.1
5′-d(GCGTA**B**ATTGCT)-3′	3753.5	3754.5
5′-d(GCGTG**B**GTTGCT)-3′	3785.5	3786.5
5′-d(GCGT**B**C**B**TTGCT)-3′	3823.5	3822.0
5′-d(GCGTC**BB**TTGCT)-3′	3823.5	3823.4
5′-d(GCGT**BBB**TTGCT)-3′	3941.6	3941.1

Evaluation of the duplex-forming abilities of BNAP

The hybridization properties of **B**-ODNs with various flanking sequences were evaluated by UV melting (T_m) experiments and the results are shown in Table 2. ODNs bearing 2′-deoxycytidine (**C**), and 2′,4′-BNA/LNA with 5-methylcytosine (**L**) and **P**, were also investigated as controls.

View Article Online
DOI: 10.1039/C7OB01874F

Table 2. T_m values of duplexes formed by ODNs with complementary (c) DNA and cRNA.

Sequences (5′-**NNN**-3′)	T_m (ΔT_m: (T_m (**L**, **P** or **B**) -T_m (**C**))) (°C)							
	Target DNA				Target RNA			
X:	**C**	**L**	**P**	**B**	**C**	**L**	**P**	**B**
T**X**T	40	44 (+4)	44 (+4)	46 (+6)	41	48 (+7)	45 (+4)	50 (+9)
C**X**A	44	48 (+4)	49 (+5)	50 (+6)	46	53 (+7)	49 (+3)	54 (+8)
C**X**C	45	51 (+6)	51 (+6)	54 (+9)	54	61 (+7)	56 (+2)	62 (+8)
A**X**A	41	45 (+4)	38 (−3)	40 (−1)	38	44 (+6)	36 (−2)	40 (+2)
G**X**G	46	48 (+2)	46 (±0)	48 (+2)	46	51 (+5)	45 (−1)	49 (+3)
XCX	45	55 (+10)	54 (+9)	59 (+14)	54	67 (+13)	59 (+5)	69 (+15)
C**XX**	45	53 (+8)	56 (+11)	57 (+12)	54	65 (+11)	64 (+10)	67 (+13)
XXX	45	58 (+13)	61 (+16)	60 (+15)	54	71 (+17)	70 (+16)	73 (+19)

UV melting profiles were measured in 2 mM sodium phosphate buffer (pH 7.2) containing 20 mM NaCl at a scan rate of 0.5 °C/min at 260 nm. The concentration of oligonucleotide used was 2 μM for each strand. The error in T_m values was ±0.5 °C.
C: 2′-deoxycytidine, **L**: 2′,4′-BNA/LNA with 5-methylcytosine, **P**: 2′-deoxyribonucleoside with phenoxazine, **B**: BNAP.
Sequence: 5′-d(GCGT**NNN**TTGCT)-3′/3′-CGC**QGQ**AACGA-5′ (**X**: **C**, **L**, **P** or **B**) (**Q**: Corresponding matching base).

First, for single modifications of **B**-ODN with complementary DNA (cDNA), the **B**-ODN/cDNA duplexes showed ΔT_m values ranging from −1°C to +9°C; unless otherwise specified, ΔT_m indicates the difference in melting temperature compared to **C**-ODN/cDNA (or cRNA) with the same sequence. Note that ODNs with specific adjacent bases are denoted as, for example, **B**-ODN(C**B**C). The highest increase in T_m value was observed for the **B**-ODN(C**B**C)/cDNA (ΔT_m: +9°C). Moreover, this T_m value was +3°C higher than those of **L**-ODN(C**L**C)/cDNA and **P**-ODN(C**P**C)/cDNA. However, **B**-ODN(A**B**A)/cDNA and **B**-ODN(G**B**G)/cDNA with 5′-flanking purine bases did not show comparable stabilization effects [ΔT_m: −1°C and +2°C, respectively], and rather exhibited T_m values lower than or equal to **L**-ODN(A**L**A)/cDNA and **L**-ODN(G**L**G)/cDNA but +2°C higher than those of **P**-ODN(A**P**A)/cDNA and **P**-ODN(G**P**G)/cDNA. Overall, the T_m values of all **P**-ODN/cDNAs were 1°C to 3°C lower than that of the corresponding **B**-ODN/cDNA. On the other hand, both **L**-ODN/cDNA and **P**-ODN/cDNA with 5′-adjacent pyrimidine bases showed almost equal T_m values [ΔT_m: +4°C to +6°C], but in the case of 5′-flanking purines, **P**-ODN/cDNAs were less stable than **L**-ODN/cDNAs. These results suggest that the sequence dependency of **B**-ODN/cDNA may be mainly due to the phenoxazine moiety.

Next, **B**-ODNs containing multiple **B** modifications were evaluated. **B**-ODN/cDNAs containing two or three **B** residues showed higher thermal stability (ΔT_m/modification: +5.0°C to +7.0°C). Moreover, interval modifications (**B**C**B**) rather than continuous modifications (C**BB** or **BBB**) resulted in larger increases in thermal stability per modification.

The duplex-forming ability of **B**-ODNs was also evaluated with complementary RNA (cRNA). With single modifications, **B**-ODN/cRNAs showed ΔT_m values ranging from +2°C to +9°C. ΔT_m values of the **B**-ODN/cRNAs bearing 5′-flanking pyrimidines were +1°C to +2°C higher than those of the corresponding **L**-ODN/cRNA. However, 5′-flanking purines resulted in decreased affinities to **B**-ODN/cRNAs compared with **L**-ODN/cRNAs (ΔT_m: −2°C to −4°C). In contrast, all **B**-ODN/cRNAs showed excellent affinities compared to **P**-ODN/cRNAs (ΔT_m: +2°C to +6°C). Overall, the ΔT_m results of **B**-ODN/cRNAs were +1°C to +3°C higher than that of **B**-ODN/cDNAs. Conversely, the ΔT_m values of **P**-ODN/cRNAs were ±0°C to −4°C, which were equal or lower than those of **P**-ODN/cDNAs. Furthermore, the π-π stacking interactions of the phenoxazine base in A-form duplexes such as DNA/RNA may be insufficient. In contrast, the ΔT_m values of the **L**-ODN/cRNAs were +1°C to +3°C higher than those of **L**-ODN/cDNAs. Adequate pre-organization of 2′,4′-BNA/LNA to the N-type sugar conformation favours DNA/RNA A-form duplex (N-type) rather than DNA/DNA B-form duplex (S-type). Thus, in the case of **B**-ODN/cRNA with 5′-flanking pyrimidines, the influence of **B** may be mainly due to the 2′,4′-BNA/LNA sugar rather than the phenoxazine base. On the contrary, in the case of **B**-ODN/cRNA with 5′-adjacent purines, the influence of the phenoxazine base in **B** increased, destabilizing the duplex.

Finally, **B**-ODN/cRNAs containing multiple modifications of **B** were evaluated. **B**-ODN/cRNAs containing two or three **B** residues showed higher thermal stability (ΔT_m/modification: +6.3°C to +7.5°C). Furthermore, as with cDNA, interval modification (**B**C**B**) rather than continuous modifications (C**BB** or **BBB**) showed higher duplex-forming abilities per modification.

Evaluation of the base selectivity of BNAP

The base discrimination ability of **B** was investigated and compared with that of **C**, **L**, and **P** (Table 3).

ODNs with the flanking sequence 5′-C**X**C-3′ (**X**: **C**, **L**, **P** or **B**), which showed effective duplex-forming abilities, were used. **B**-ODN showed excellent discrimination toward C compared with **C**-ODN, **L**-ODN and **P**-ODN [ΔT_m(G-C): −28°C (**B**-ODN)], and the discrimination of **B**-ODN toward A and T was similar to those of **C**-ODN and **L**-ODN [ΔT_m(G-A): −15°C (**B**-ODN), ΔT_m(G-T): −15°C (**B**-ODN)]. On the other hand, **P**-ODN showed lower base

discrimination towards T compared with **C**-ODN, **L**-ODN and **P**-ODN [ΔT_m (G-T): −12°C (**P**-ODN)], whereas **P**-ODN exhibited similar discrimination towards A and C [ΔT_m(G-A): −12°C (**P**-ODN), ΔT_m(G-C): −23°C (**P**-ODN)] as did **C**-ODN and **L**-ODN. These findings strongly support the hypothesis that the 2′,4′-BNA/LNA moiety in **B** compensates for the low selectivity of the phenoxazine base toward the targeted T, and the superior base discrimination of **B** toward the targeted C is due to new properties acquired via the fusion of 2′,4′-BNA/LNA and phenoxazine.

The base discrimination of **B** towards cRNA was also investigated (see Supporting Information, Table S2) and was found to exhibit efficient base selectivity.

Table 3. Comparison of matched versus mismatched hybridization

5′-d(GCGTC**X**CTTGCT)-3′
3′-d(CGCAG**Y**GAACGA)-5′

X =	T_m (ΔT_m: T_m[mismatch]-T_m[match]) (°C)			
Y =	G	A	T	C
C	45	32 (−13)	29 (−16)	24 (−21)
L	51	37 (−14)	33 (−18)	27 (−24)
P	51	39 (−12)	39 (−12)	28 (−23)
B	54	39 (−15)	39 (−15)	26 (−28)

Values in parentheses are the difference between the T_m when the ODN was bound with the guanine-containing target and the T_m when the ODN was bound with a mismatched base. The buffer conditions were the same as given in Table 2. **C**: 2′-deoxycytidine, **L**: 2′,4′-BNA/LNA with 5-methylcytosine, **P**: 2′-deoxyribonucleoside with phenoxazine, **B**: BNAP.

CD measurements of duplexes containing BNAP

The duplex structures of **B** were analysed by circular dichroism (CD) measurements (Figure 2). The **C**-ODN/cDNA and **C**-ODN/cRNA duplexes produced typical spectra of B- and A-type helices, respectively. The incorporation of each modification (**L**, **P**, and **B**) into DNA/DNA and DNA/RNA duplexes resulted in no significant change in the CD spectra, which suggests that these modifications do not induce significant change in duplex structure. Some small changes were observed: for example, the **P**-ODN/cDNA and **B**-ODN/cDNA duplexes exhibited a unique small negative Cotton band at 230–240 nm. Conversely, the CD patterns of both **P**-ODN/cRNA and **B**-ODN/cRNA duplexes were similar in the 220–240 nm region, and different from those of duplexes containing **C** and **L**. Thus, the CD spectrum around 220–240 nm may exhibit features derived from the phenoxazine base.

Thermodynamic parameters of ODNs containing BNAP

A detailed thermodynamic analysis was conducted to determine whether the 2′,4′-BNA/LNA sugar or the phenoxazine base in BNAP predominantly contributes to the function of BNAP. The analysis of duplexes with 5′-CXC-3′ was conducted by constructing van't Hoff plots based on T_m results obtained at various concentrations (Table 3, see also Supporting Information, Figure S6).

For duplexes with cDNA, **B**-ODN/cDNA showed a small favourable entropy change ($\Delta\Delta H$ = +2.2 kcal/mol, $\Delta\Delta S$: +14 cal/mol·K). [$\Delta\Delta H$, $\Delta\Delta S$ or $\Delta\Delta G$ indicate the difference with the corresponding ΔH, ΔS or ΔG values obtained for **C**-ODN/cDNA (or cRNA).] In contrast, **L**-ODN/cDNA showed a favourable large entropy change though significant enthalpy loss was observed ($\Delta\Delta H$: +15.1 kcal/mol, $\Delta\Delta S$: +52 cal/mol·K), and **P**-ODN/cDNA showed small enthalpy and entropy changes ($\Delta\Delta H$: −0.9 kcal/mol, $\Delta\Delta S$: +2 cal/mol·K). Based on these results, the ΔS and ΔH changes of **B**-ODN/cDNA are similar to those of **P**-ODN/cDNA rather than those of **L**-ODN/cDNA. The ΔG (Gibbs' free energy change) of **L**-ODN/cDNA was small ($\Delta\Delta G$: −1.1 kcal/mol), whereas **P**-ODN/cDNA and **B**-ODN/cDNA showed high stability ($\Delta\Delta G$: −1.6

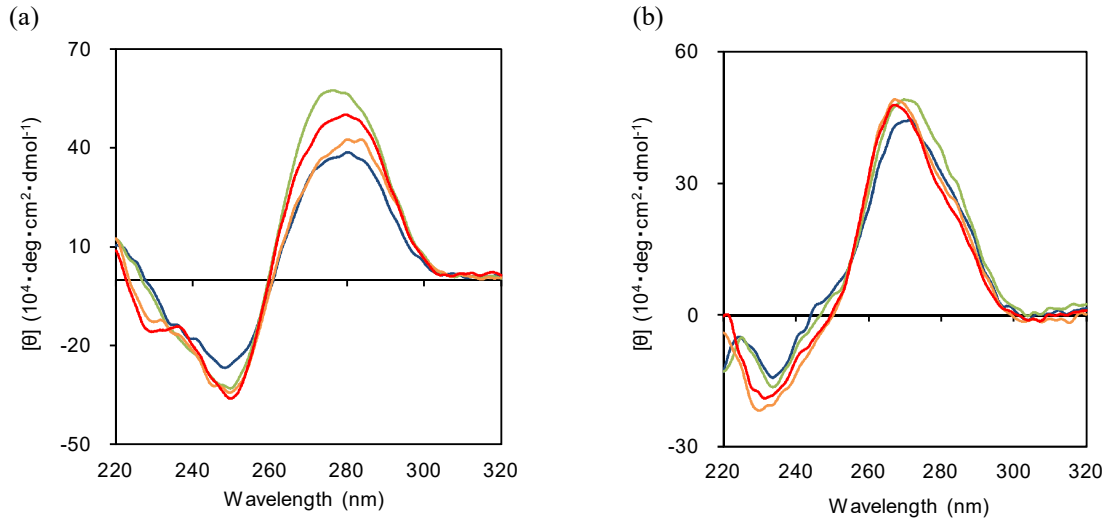

Figure 2. CD spectra of DNA/DNA (panel a) and DNA/RNA (panel b) duplexes.

Conditions: 2 mM sodium phosphate buffer (pH 7.2), 20 mM NaCl, 2 μM each strand. **C**: 2′-deoxycytidine (blue), **L**: 2′,4′-BNA/LNA with 5-methylcytosine (green), **P**: 2′-deoxyribonucleoside with phenoxazine (orange), **B**: BNAP (red).
Sequence: 5′-d(GCGT**CXC**TTGCT)-3′/3′-CGC**GCG**AACGA-5′ (**X**: **C**, **L**, **P** or **B**).

View Article Online
DOI: 10.1039/C7OB01874F

Table 3. Thermodynamic parameters of duplexes with cDNA and cRNA.

X =	Target DNA						Target RNA					
	ΔH	ΔS	$\Delta G_{(37°C)}$	$\Delta\Delta H$	$\Delta\Delta S$	$\Delta\Delta G_{(37°C)}$	ΔH	ΔS	$\Delta G_{(37°C)}$	$\Delta\Delta H$	$\Delta\Delta S$	$\Delta\Delta G_{(37°C)}$
C	−93.3	−265	−11.0	-	-	-	−97.4	−271	−13.4	-	-	-
L	−78.2	−213	−12.1	+15.1	+52	−1.1	−104.6	−286	−16.0	−7.2	−15	−2.6
P	−94.2	−263	−12.6	−0.9	+2	−1.6	−96.0	−264	−14.1	+1.4	+7	−0.7
B	−91.1	−251	−13.4	+2.2	+14	−2.4	−109.8	−300	−16.7	−12.4	−29	−3.3

C: 2′-deoxycytidine, **L**: 2′,4′-BNA/LNA with 5-methylcytosine, **P**: 2′-deoxyribonucleoside with phenoxazine, **B**: BNAP.
Sequence: 5′-d(GCGTC**X**CTTGCT)-3′/3′-CGCG**C**GAACGA-5′ (**X**: **C**, **L**, **P** or **B**).
The units of ΔH, ΔS and ΔG are kcal/mol, cal/mol·K and kcal/mol, respectively. $\Delta\Delta H$, $\Delta\Delta S$ and $\Delta\Delta G$ indicate the difference of the corresponding ΔH, ΔS and ΔG value from that of **C**-ODN/cDNA (or cRNA) duplex.

and −2.4 kcal/mol, respectively). Thus, the thermodynamic parameters of **B**-ODN/cDNA were similar to those of **P**-ODN/cDNA rather than those of **L**-ODN/cDNA, indicating that the phenoxazine base in BNAP predominantly works within the DNA/DNA duplex (ODN/cDNA).

Next, thermodynamic analysis was conducted with cRNA. **B**-ODN/cRNA showed the most favourable enthalpy change ($\Delta\Delta H$: −12.4 kcal/mol, $\Delta\Delta S$: −29 cal/mol·K). **L**-ODN/cRNA and **P**-ODN/cRNA showed a favourable enthalpy change and a small favourable entropy change, respectively. Furthermore, the $\Delta\Delta G$ of **B**-ODN/cRNA (−3.3 kcal/mol) was similar to that of **L**-ODN/cRNA (−2.6 kcal/mol) but significantly different from the $\Delta\Delta G$ of **P**-ODN/cRNA (−0.7 kcal/mol). In DNA/RNA (ODN/cRNA), unlike DNA/DNA, the thermodynamic parameters of **B**-ODN/cDNA were similar to that of **L**-ODN/cRNA rather than that of **P**-ODN/cRNA.

Thus, in the above sequences with 5′-C**X**C-3′, the phenoxazine moiety in BNAP mainly affects the duplex-forming ability of DNA/DNA, and conversely, the 2′,4′-BNA/LNA moiety predominantly influences the duplex forming ability of DNA/RNA.

Thermodynamic analysis of duplexes with 5′-A**B**A-3′ (see Supporting Information, Table S3) showed that the thermodynamic parameters of duplex formed with **B**-ODN(A**B**A) and duplex formed with **B**-ODN(C**B**C) were completely different. These results revealed that the thermodynamic parameters of **B**-ODN depend significantly on the flanking sequence.

Discussion

Modifications of the phenoxazine base in oligonucleotide significantly improve its duplex-forming ability due to effective π-π stacking between adjacent nucleobases.[10a,b] This π-π stacking interaction has been confirmed by molecular modeling[10a,b] and X-ray analysis[16] using phenoxazine and its analogues. **B**-ODN with 5′-flanking pyrimidine bases showed much better binding affinity than did the corresponding **L**-ODN and **P**-ODN due to the π-π stacking interaction between the phenoxazine base and the pyrimidine, whereas this interaction did not stabilize duplexes if the **B**-ODN contained 5′-flanking purine sequences. The π-π stacking interaction of the phenoxazine base functions well in B-type duplex such as DNA/DNA[10b] but poorly in A-type duplex such as DNA/RNA.[10a] Conformational change of the duplex significantly affects π-π overlap between phenoxazine and the 5′-flanking nucleobase. Therefore, the thermal stability of **B** is largely dependent on the duplex-structure and flanking sequence. During the design of BNAP, we anticipated a powerful additive effect, without loss of affinity, resulting from the fusion of 2′,4′-BNA/LNA and phenoxazine. BNAP exhibits greatly enhanced duplex-forming ability compared to 2′,4′-BNA/LNA, but this ability is not equivalent to the summed ability exhibited by 2′,4′-BNA/LNA and phenoxazine. This lack of additivity suggests that (a) the spatial position of phenoxazine base fixed by 2′,4′-BNA/LNA sugar modification in **B** is not completely fit for duplex structures, and/or (b) the stabilization mechanisms of both modifications partially overlap. It has been reported that the duplex-forming ability of 2′,4′-BNA/LNA might be due to π-π stacking interactions,[17] similar to that of phenoxazine base.

Thermodynamic analysis (ΔH, ΔS and ΔG) clearly revealed that in the sequence 5′-C**X**C-3′, BNAP exhibits properties associated with the phenoxazine moiety in DNA/DNA duplex and characteristics associated with the 2′,4′-BNA/LNA moiety in DNA/RNA duplex. It is interesting that the predominance of each characteristic changed depending on whether the duplex-structure was DNA/DNA or DNA/RNA.

Conclusions

In conclusion, we demonstrated the synthesis and evaluation of 2′,4′-BNA/LNA bearing a phenoxazine base. **B**-ODN showed superior duplex-forming abilities compared to **C**-ODN, **L**-ODN, and **P**-ODN. Thermodynamic analysis of **B** revealed that the phenoxazine moiety is dominant in DNA/DNA duplex and that the 2′,4′-BNA/LNA moiety is dominant in DNA/RNA duplex. Thus, BNAP is a promising candidate for oligonucleotide therapeutics and DNA nanotechnologies, especially for those requiring high duplex-forming ability. The synthesis and evaluation of 2′,4′-BNA/LNA with a 9-(aminoethoxy)phenoxazine (G-clamp) base are now underway for further improvement of the duplex-forming ability.

View Article Online
DOI: 10.1039/C7OB01874F

Experimental

General

Dry dichloromethane, *N*,*N*-dimethylformamide, tetrahydrofuran, acetonitrile and pyridine were used as purchased. ^{1}H-, ^{13}C- and ^{31}P NMR spectra were recorded on JEOL JNM-ECS300, JNM-ECS400 and JNM-ECA500 spectrometers. Chemical shift values are expressed in δ values (ppm) relative to internal tetramethylsilane (0.00 ppm), CHD_2OD (3.30 ppm) or $CHD_2S(=O)CD_3$ (2.50 ppm) for ^{1}H NMR, chloroform-d_1 (77.0 ppm) or DMSO-d_6 (39.5 ppm) for ^{13}C NMR, and 1% H_3PO_4 (0.00 ppm) for ^{31}P-NMR. IR spectra were recorded on a JASCO FT/IR-4200 spectrometer. Optical rotations were recorded on a JASCO DIP-370 instrument. MALDI-TOF mass spectra of all new compounds were measured on a JEOL SpiralTOF JMS-S3000. MALDI-TOF mass spectra of ODNs were measured on a Bruker Daltonics Autoflex II TOF/TOF mass spectrometer. Fuji Silysia PSQ-60B or PSQ-100B silica gel was used for column chromatography.

3′,5′-di-*O*-Acetyl-2′-*O*,4′-*C*-methyleneuridine (3)

To a solution of compound **2** (139 mg, 0.54 mmol) in pyridine (2 ml) was added acetic anhydride (110 μL, 1.16 mmol) at 0°C, and the resultant mixture was stirred at room temperature for 7 h. After addition of saturated aqueous $NaHCO_3$ solution, the solution was extracted with AcOEt. The organic extracts were washed with saturated aqueous $NaHCO_3$ solution, dried over Na_2SO_4, and concentrated under reduced pressure. The residue was purified by silica gel column chromatography (*n*-hexane/AcOEt = 1/2 to 1/3) to give compound **3** (183 mg, 99%) as a white foam. $[\alpha]_D^{28}$ +68.7 (*c* 0.3, $CHCl_3$); IR ν_{max} (KBr): 3524, 3167, 3055, 1748, 1687, 1455, 1374, 1234, 1110, 1083, 1049 cm^{-1}; ^{1}H NMR (500 MHz, $CDCl_3$): δ 2.14 (3H, s), 2.15 (3H, s), 3.99, 4.04 (2H, AB, *J* = 8 Hz), 4.40, 4.50 (2H, AB, *J* = 13 Hz), 4.69 (1H, s), 4.86 (1H, s), 5.71 (1H, s), 5.79 (1H, d, *J* = 8 Hz), 7.60 (1H, d, *J* = 8 Hz); ^{13}C NMR (126 MHz, $CDCl_3$): δ 20.6, 20.7, 58.8, 71.1, 71.8, 77.9, 85.6, 87.2, 102.4, 137.9, 149.7, 163.0, 169.7, 170.1; HRMS (MALDI) calcd. for $C_{14}H_{16}N_2NaO_8$ $[M+Na]^+$: 363.0799, found: 363.0791.

5-Bromo-3′,5′-di-*O*-acetyl-2′-*O*,4′-*C*-methyleneuridine (4)

To a solution of compound **3** (6.69 g, 19.7 mmol) in anhydrous *N*,*N*-dimethylformamide (DMF) (190 ml) was added *N*-bromosuccinimide (NBS) (5.24 g, 29.0 mmol) at 0°C, and the resultant mixture was stirred at 0°C for 1.5 h under an Ar atmosphere, then stirred at room temperature for 1 h. After removal of DMF *in vacuo* with heat, the residue was purified by silica gel column chromatography (CH_3Cl/MeOH = 97/3) to give compound **4** (6.45 g, 81%) as a white solid. $[\alpha]_D^{27}$ +3.5 (*c* 0.4, $CHCl_3$); IR ν_{max} (KBr): 3525, 3190, 3084, 2823, 1749, 1697, 1619, 1438, 1370, 1232, 1133, 1094, 1056 cm^{-1}; ^{1}H NMR (500 MHz, $CDCl_3$): δ 2.15 (3H, s), 2.24 (3H, s), 3.96, 4.03 (2H, AB, *J* = 8 Hz), 4.41, 4.46 (2H, AB, *J* = 13 Hz), 4.68 (1H, s), 4.86 (1H, s), 5.68 (1H, s), 7.99 (1H, s), 8.56 (1H, brs); ^{13}C NMR (126 MHz, DMSO-d_6): δ 20.5, 20.6, 58.8, 70.8, 71.2, 77.4, 85.4, 86.7, 95.8, 138.2, 149.4, 159.3, 169.6, 169.8; HRMS (MALDI) calcd. for $C_{14}H_{15}{}^{79}BrN_2NaO_8$ $[M+Na]^+$: 440.9904, found: 440.9903.

5-Bromo-*N*^{4}-(2-hydroxyphenyl)- 2′-*O*,4′-*C*-methylenecytidine (6)

To a solution of compound **4** (850 mg, 2.00 mmol) in CH_2Cl_2 (90 ml) was added triphenylphosphine (Ph_3P), then CCl_4 (20 ml) was added. The resultant mixture was refluxed for 2 h under an Ar atmosphere, then cooled to room temperature. 2-Aminophenol (533 mg, 4.88 mmol) and 1,8-diazabicyclo[5.4.0]undec-7-ene (DBU) (600 μl, 4.01 mmol) were added, and the mixture was stirred at room temperature for 12 h. The reaction mixture was concentrated under reduced pressure and the residue was dissolved in CH_3Cl. This organic layer was washed with 5% citric acid aqueous solution, dried over Na_2SO_4, and concentrated under reduced pressure. The residue was quickly passed through a short silica gel column (*n*-hexane/AcOEt = 1/1 to 1/2). Without further purification, compound **5** contaminated with Ph_3P=O (1.93 g) was dissolved in 7 M NH_3 in MeOH (12 ml) and the reaction mixture was stirred at room temperature for 2 h. The mixture was then concentrated to remove MeOH under reduced pressure and the residue was purified by silica gel column chromatography (*n*-hexane/AcOEt = 1/3 to 0/1) to give compound **6** (693 mg, 81% in 2 steps) as a white solid. $[\alpha]_D^{25}$ +84.6 (*c* 0.1, 1,4-dioxane); IR ν_{max} (KBr): 3355, 2956, n 1716, 1646, 1618, 1558, 1494, 1460, 1290, 1232, 1117, 1083, 1051 cm^{-1}; ^{1}H NMR (500 MHz, CD_3OD): δ 3.76, 3.96 (2H, AB, *J* = 8 Hz), 3.89, 3.92 (2H, AB, *J* = 13 Hz), 4.05 (1H, s), 4.36 (1H, s), 5.58 (1H, s), 6.85 (1H, t, *J* = 8 Hz), 6.86 (1H, d, *J* = 8 Hz), 6.99 (1H, t, *J* = 8 Hz), 8.28 (1H, s), 8.40 (1H, d, *J* = 8 Hz); ^{13}C NMR (101 MHz, DMSO-d_6): δ 55.6, 68.2, 71.0, 78.6, 87.1, 87.8, 89.0, 115.0, 119.1, 122.3, 125.2, 125.9, 140.7, 148.2, 152.9, 157.4; HRMS (MALDI) calcd. for $C_{16}H_{16}{}^{79}BrN_3NaO_6$ $[M+Na]^+$: 448.0115, found: 448.0113.

1,3-Diaza-3-(2′-*O*,4′-*C*-methylene-β-D-ribofuranosyl)-2-oxophenoxazine (7)

To a solution of compound **6** (1.20 g, 2.80 mmol) in EtOH (300 ml) was added DBU (460 μl, 3.08 mmol) and the resultant mixture was refluxed for 30 h. The reaction mixture was concentrated under reduced pressure. After precipitation with MeOH, the residue was purified by silica gel column chromatography (AcOEt/MeOH = 1/0 to 9/1) to give compound **7** (569 mg, 59%) as an orange solid. $[\alpha]_D^{26}$ −76.7 (*c* 0.1, EtOH); IR ν_{max} (KBr): 3392, 3299, 2961, 2362, 2338, 2328, 1677, 1636, 1577, 1508, 1472, 1421, 1337, 1260, 1231, 1085, 1049 cm^{-1}; ^{1}H NMR (500 MHz, DMSO-d_6): δ 3.60, 3.80 (2H, AB, *J* = 8 Hz), 3.73 (2H, s), 3.92 (1H, s), 4.11 (1H, s), 5.27 (1H, brs), 5.34 (1H, s), 5.68 (1H, brs), 6.78-6.89 (4H, m), 7.45 (1H, s), 10.6 (1H, brs); ^{13}C NMR (101 MHz, DMSO-d_6): δ 55.7, 68.3, 70.9, 78.8, 86.6, 88.8, 115.2, 116.6, 121.3, 123.7, 123.8, 126.9, 127.2, 142.2, 152.6, 154.0; HRMS (MALDI) calcd. for $C_{16}H_{16}N_3O_6$ $[M+H]^+$: 346.1034, found: 346.1027.

1,3-Diaza-3-[5′-*O*-(4,4′-dimethoxytrityl)-2′-*O*,4′-*C*-methylene-β-D-ribofuranosyl]-2-oxophenoxazine (8)

To a solution of silver trifluoromethanesulfonate (AgOTf) (364 mg, 1.42 mmol) in CH_2Cl_2 (5 ml) was added 4,4′-dimethoxy chloride (DMTrCl) (515 mg, 1.52 mmol) in CH_2Cl_2 (5 ml), and the resultant mixture was stirred for 1 h at room temperature under an Ar atmosphere to give DMTrOTf solution. Then, to a solution of compound **7** (99 mg, 0.28 mmol) in anhydrous 2,6-lutidine (8 ml) was added DMTrOTf solution (4.8 ml) at 0°C, and the mixture was

stirred for 3 h. After addition of $NaHCO_3$ aq. at 0°C, the mixture was extracted with AcOEt. The organic layer was washed with saturated aqueous $NaHCO_3$ solution and copper (II) sulphate aqueous solution (3.00 g in 20 ml H_2O), dried over Na_2SO_4, and then concentrated under reduced pressure. The residue was purified by silica gel column chromatography (0.5% triethylamine in *n*-hexane/AcOEt = 1/9 to 0/1) to give compound **8** (105 mg, 58%) as a yellow foam. $[\alpha]_D^{27}$ −82.0 (*c* 0.3, $CHCl_3$); IR ν_{max} (KBr): 3413, 3086, 2952, 2838, 2357, 2334, 1677, 1640, 1607, 1576, 1499, 1472, 1419, 1331, 1282, 1254, 1178, 1082, 1048 cm^{-1}; ^1H NMR (500 MHz, $CDCl_3$): δ 3.44 (2H, s), 3.73, 3.88 (2H, AB, *J* = 7 Hz), 3.78 (3H, s), 3.79 (3H, s), 4.08 (1H, brs), 4.40 (1H, s), 4.78 (1H, s), 5.63 (1H, s), 6.60-6.68 (3H, m), 6.87 (4H, dd, *J* = 3, 9 Hz), 7.05 (1H, s), 7.20 (1H, t, *J* = 7 Hz), 7.33 (2H, t, *J* = 8 Hz), 7.37 (4H, dd, *J* = 2, 9 Hz), 7.48 (2H, d, *J* = 8 Hz), 7.73 (1H, s), 11.2 (1H, brs); ^{13}C NMR (101 MHz, $CDCl_3$): δ 55.2, 58.6, 70.3, 72.1, 79.9, 86.5, 87.2, 87.8, 113.3, 114.7, 118.0, 120.2, 123.3, 124.2, 126.5, 126.8, 127.5, 127.9, 128.0, 130.1, 130.2, 135.2, 135.4, 142.5, 144.9, 153.3, 155.3, 158.5, 158.5; HRMS (MALDI) calcd. for $C_{37}H_{33}N_3NaO_8$ $[M+Na]^+$: 670.2160, found: 670.2162.

1,3-Diaza-3-[3′-*O*-(*N*,*N*-diisopropylamino-2-cyanoethoxyphosphino)-5′-*O*-(4,4′-dimethoxytrityl)-2′-*O*,4′-*C*-methylene-β-D-ribofuranosyl]-2-oxophenoxazine (9)

To a solution of compound **8** (107 mg, 0.160 mmol) in CH_2Cl_2 (1 ml) was added *N*,*N*-diisopropylethylamine (DIPEA) (85 µl, 0.48 mmol) and 2-cyanoethyl *N*,*N*-diisopropylchlorophosphoramidite (80 µl, 0.36 mmol) at 0°C and the mixture was stirred for 3 h at room temperature under an Ar atmosphere. After addition of saturated aqueous $NaHCO_3$ solution at 0°C, the mixture was extracted with AcOEt. The organic layer was washed with saturated aqueous $NaHCO_3$ solution, water, and brine, dried over Na_2SO_4, and then concentrated under reduced pressure. The residue was purified by silica gel column chromatography (0.5% triethylamine in *n*-hexane/AcOEt = 1/1 to 3/7) to give compound **9** (100 mg, 74%) as a yellow foam. ^1H NMR (300 MHz, $CDCl_3$): δ 0.99-1.29 (13H, m), 2.38 (13/20H, t, *J* = 7 Hz), 2.54 (7/20H, t, *J* = 6 Hz), 3.35-3.85 (14H, m), 4.28 (7/20H, d, *J* = 12 Hz), 4.39 (13/20H, d, *J* = 15 Hz), 4.65 (13/20H, s), 4.72 (7/20H, s), 5.72 (1H, s), 6.55-6.59 (1H, m), 6.80-6.92 (6H, m), 7.25-7.41 (7H, m), 7.47-7.64 (4H, m); ^{31}P NMR (203 MHz, $CDCl_3$): δ 149.1, 149.2; HRMS (MALDI) calcd. for $C_{46}H_{50}N_5NaO_9P$ $[M+Na]^+$: 870.3238, found: 870.3240.

Synthesis of the ODNs containing BNAP

The ODNs containing BNAP were synthesized using an automated DNA/RNA (Gene Design, nS-8) Nucleic Acid Synthesis System at 0.2 or 1.0 mmol scale. 5-[3,5-Bis(trifluoromethyl)phenyl]-1*H*-tetrazole (Activator 42®) was used for all coupling steps as the activator. The standard phosphoramidite protocol coupling time of 70 s was increased to 15 min. The BNAP phosphoramidite **13** was prepared in 0.1 M acetonitrile solution. The ODN syntheses were performed using DMTr-on mode. Solid (CPG)-supported ODNs were cleaved and the protecting groups on each nucleobase were removed with a mixture of aqueous methylamine (40%) and aqueous ammonia (28%) solution (v/v, 1/1) at 65°C for 10 min. The crude ODNs bearing a DMTr group were detritylated and purified using a Sep-Pak® Plus C18 Cartridge and a Sep-Pak® Plus C18 Environmental Cartridge, washed with 10% MeCN aqueous solution, detritylated with 0.5% aqueous trifluoroacetic acid solution, and eluted with 35% aqueous MeOH solution. The product was subjected to reverse-phase HPLC using a Waters XBridge™ OST C18 2.5 µm (10 × 50 mm) column using 0.1 M triethylammonium acetate (TEAA) buffer (pH 7.0) as buffer A and 50% MeCN in 0.1 M TEAA buffer (pH 7.0) as buffer B. The purity of the ODNs was confirmed by reverse-phase HPLC using a Waters XBridge™ OST C18 2.5 µm (4.6 × 50 mm) column and by MALDI-TOF mass spectrometry.

UV melting experiments (T_m measurements)

UV melting experiments were carried out on SHIMADZU UV-1650PC and UV-1800 spectrometers equipped with T_m analysis accessory quartz cuvettes with 1 cm optical path lengths. The UV melting profiles were recorded in 2 mM sodium phosphate buffer (pH 7.2) containing 20 mM NaCl to give a final strand concentration of 2 µM. The samples were annealed by heating at 100°C, followed by slow cooling to room temperature. The melting profile was recorded at 260 nm from 5 to 90°C at a scan rate of 0.5°C /min. A two-point average method was used to obtain the T_m values and the final values were determined by averaging three independent measurements which were accurate to within 1°C.

CD measurements

CD spectra were measured using a JASCO J-720W spectrophotometer. The spectra were recorded at 10°C in a quartz cuvette with a 1 cm optical path length. The samples were prepared in the same manner as described for the UV melting experiments. The molar ellipticity was calculated from the equation $[\theta] = \theta/cl$, where θ is the relative intensity, *c* is the sample concentration, and *l* is the cell path length in centimetres.

Conflicts of interest

There are no conflicts of interest to declare.

Acknowledgements

This work was supported by the Core Research for Evolutional Science and Technology (CREST) program of the Japan Science and Technology Agency (JST), and JSPS KAKENHI Grant Number 15K08024. This research was also partially supported by the Platform Project for Supporting Drug Discovery and Life Science Research from the Japan Agency for Medical Research and Development (AMED).

Notes and references

1. K. Morihiro, Y. Kasahara and S. Obika, *Mol. BioSyst.*, 2017, **13**, 235-245.
2. (a) S. Obika, D. Nanbu, Y. Hari, K. Morio, Y. In, T. Ishida and T. Imanishi, *Tetrahedron Lett.*, 1997, **38**, 8735-8738; (b) S. Obika, D. Nanbu, Y. Hari, J. Andoh, K. Morio, T. Doi and T. Imanishi, *Tetrahedron Lett.*, 1998, **39**, 5401–5404.
3. (a) S. K. Singh, P. Nielsen, A. A. Koshkin and J. Wengel, *Chem. Commun.*, 1998, 455-456; (b) A. A. Koshkin, S. K.

Singh, P. Nielsen, V. K. Rajwanshi, R. Kumar, M. Meldgaard, C. E. Olsen and J. Wengel, *Tetrahedron*, 1998, **54**, 3607-3630.

4. (a) A. Yahara, A. R. Shrestha, T. Yamamoto, Y. Hari, T. Osawa, M. Yamaguchi, M. Nishida, T. Kodama and S. Obika, *ChemBioChem*, 2012, **13**, 2513-2516; (b) T. Yamamoto, A. Yahara, R. Waki, H. Yasuhara, F. Wada, M. Harada-Shiba and S. Obika, *Organic Biomol. Chem.*, 2015, **13**, 3757-3765.
5. A. R. Shrestha, Y. Kotobuki, Y. Hari and S. Obika, *Chem. Commun.*, 2014, **50**, 575-577.
6. (a) T. Yamaguchi, M. Horiba and S. Obika, *Chem. Commun.*, 2015, **51**, 9737-9740; (b) M. Horiba, T. Yamaguchi and S. Obika, *J. Org. Chem.*, 2016, **81**, 11000-11008.
7. K. Morihiro, T. Kodama, Kentefu, Y. Moai, R. N. Veedu and S. Obika, *Angew. Chem. Int. Ed.,* 2013, **52**, 5074-5078.
8. (a) M. Carlucci, E. Kierzek, A. Olejnik, D. H. Turner and R. Kierzek, *Biochemistry*, 2009, **48**, 10882-10893; (b) M. E. Ostergaard, P. Kumar, B. Baral, D. C. Guenther, B. A. Anderson, F. M. Ytreberg, L. Deobald, A. J. Paszczynski, P. K. Sharma and P. J. Hrdlicka, *Chem. Eur. J.*, 2011, **17**, 3157-3165; (c) M. Kaura, P. Kumar and P. J. Hrdlicka, *J. Org. Chem.*, 2014, **79**, 6256-6268; (d) T. Hara, T. Kodama, Y. Takegaki, K. Morihiro, K. R. Ito and S. Obika, *J. Org. Chem.*, 2017, **82**, 25-36.
9. (a) S. Obika, Y. Hari, M. Sekiguchi and T. Imanishi, *Angew. Chem. Int. Ed.,* 2001, **40**, 2079-2081; (b) Y. Hari, M. Akabane and S. Obika, *Chem. Commun.*, 2013, **49**, 7421-7423; (c) M. Akabane-Nakata, S. Obika and Y. Hari, *Organic Biomol. Chem.*, 2014, **12**, 9011-9015; (d) Y. Hari and S. Obika, *Nucleic Acids and Molecular Biology*, *chapter: Modified Nucleic Acids, Springer, New York*, 2016, **31**, 209-219.
10. (a) K. -Y. Lin, R. J. Jones and M. Matteucci, *J. Am. Chem. Soc.*, 1995, **117**, 3873-3874; (b) J. -A. Ortega, J. R. Blas, M. Orozco, A. Grandas, E. Pedroso and J. Robles, *Organic Lett.*, 2007, **9**, 4503-4506. (c) W. M. Flanagan, R. W. Wagner, D. Grant, K. -Y. Lin and M. D. Matteucci, *Nat. Biotech.*, 1999, **17**, 48-52.
11. (a) L. M. Wilhelmsson, A. Holmén, P. Lincoln, P. E. Nielsen and B. Nordén, *J. Am. Chem. Soc.*, 2001, **123**, 2434-2435; (b) L. M. Wilhelmsson, P. Sandin, A. Holmén, B. Albinsson, P. Lincoln and B. Nordén, *J. Phys. Chem. B*, 2003, **107**, 9094-9101; (c) K. C. Engman, P. Sandin, S. Osborne, T. Brown, M. Billeter, P. Lincoln, B. Nordén, B. Albinsson and L. M. Wilhelmsson, *Nucleic Acids Res.*, 2004, **32**, 5087-5095; (d) P. Sandin, L. M. Wilhelmsson, P. Lincoln, V. E. C. Powers, T. Brown and B. Albinsson, *Nucleic Acids Res.*, 2005, **33**, 5019-5025; (e) P. Sandin, P. Lincoln, T. Brown and L. M. Wilhelmsson, *Nat. Protoc.*, 2007, **2**, 615-623; (f) P. Sandin, K. Börjesson, H. Li, J. Mårtensson, T. Brown, L. M. Wilhelmsson and B. Albinsson, *Nucleic Acids Res.,* 2008, **36**, 157-167; (g) K. Börjesson, S. Preus, A. H. El-Sagheer, T. Brown, B. Albinsson and L. M. Wilhelmsson, *J. Am. Chem. Soc.*, 2009, **131**, 4288–4293; (h) H. Gardarsson, A. S. Kale and S. T. Sigurdsson, *ChemBioChem*, 2011, **12**, 567-575.
12. M. A. Maier, J. M. Leeds, G. Balow, R. H. Springer, R. Bharadwaj and M. Manoharan, *Biochemistry*, 2002, **41**, 1323-1327.
13. (a) G. Stengel, J. P. Gill, P. Sandin, L. M. Wilhelmsson, B. Albinsson, B. Nordén and D. Millar, *Biochemistry*, 2007, **46**, 12289-12297; (b) J. M. Walsh, I. Bouamaied, T. Brown, L. M. Wilhelmsson and P. J. Beuning, *J. Mol. Chem.*, 2011, **409**, 89-100; (c) A. Shivalingam, A. E. S. Tyburn, A. H. El-Sagheer and T. Brown, *J. Am. Chem. Soc.*, 2017, **139**, 1575-1583.
14. (a) K. -Y. Lin and M. D. Matteucci, *J. Am. Chem. Soc.*, 1998, **120**, 8531-8532; (b) W. M. Flanagan, J. J. Wolf, P. Olson, D. Grant, K. -Y. Lin, R. W. Wagner and M. D. Matteucci, *Proc. Natl. Acad. Sci. USA*, 1999, **96**, 3513-3518; (c) S. C. Holmes, A. A. Arzumanov and M. J. Gait, *Nucleic Acids Res.*, 2003, **31**, 2759-2768; (d) R. Stanton, S. Sciabola, C. Salatto, Y. Weng, D. Moshinsky, J. Little, E. Walters, J. Kreeger, D. DiMattia, T. Chen, T. Clark, M. Liu, J. Qian, M. Roy and R. Dullea, *Nucleic Acid Ther.*, 2012, **22**, 344-359.
15. (a) A. A. Koshkin, J. Fensholdt, H. M. Pfundheller, C. Lomholt, *J. Org. Chem.*, 2001, **66**, 8504-8512; (b) S. Obika, T. Uneda, T. Sugimoto, D. Nanbu, T. Minami, T. Doi and T. Imanishi, *Bioorg. Med. Chem.*, 2001, **9**, 1001-1011.
16. (a) C. J. Wilds, M. A. Maier, V. Tereshko, M. Manoharan and M. Egli, *Angew. Chem. Int. Ed.*, 2002, **41**, 115-117; (b) M. Manoharan and M. Egli, *Helv. Chemica Acta*, 2003, **86**, 966-978.
17. (a) P. M. McTigue, R. J. Peterson and J. D. Kahn, *Biochemistry*, 2004, **43**, 5388-5405; (b) H. Kaur, A. Arora, J. Wengel and S. Maiti, *Biochemistry*, 2006, **45**, 7347-7355; (c) U. Christensen, *Biosci. Rep.*, 2007, **27**, 327-333; (d) H. Kaur, J. Wengel and S. Maiti, *Biochemistry*, 2008, **47**, 1218-1227; (e) E. Kierzek, A. Pasternak, K. Pasternak, Z. Gdaniec, I. Yildirim, D. H. Turner and R. Kierzek, *Biochemistry*, 2009, **48**, 4377-4387.

View Article Online
DOI: 10.1039/C7OB01874F

Table of contents

Synthesis and thermal stabilities of oligonucleotides containing 2′-*O*,4′-*C*-methylene bridged nucleic acid with a phenoxazine base

Yuki Kishimoto, Akane Fujii, Osamu Nakagawa,* Tetsuya Nagata, Takanori Yokota, Yoshiyuki Hari and Satoshi Obika*

BNAP-modified ODNs showed higher binding affinities toward complementary DNA and RNA as compared to ODNs bearing 2′,4′-BNA/LNA with 5-methylcytosine or 2′-deoxyribonucleoside with phenoxazine.

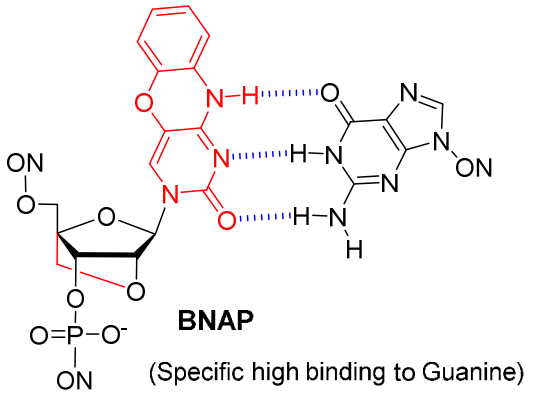

BNAP

(Specific high binding to Guanine)